A First Principle Study of Antifluorite Be_2X (X = C, Si) Polymorph

H.-Y. Yan[a], Q. Wei[b,*], S.-M. Chang[c] and P. Guo[d]

[a]Department of Chemistry and Chemical Engineering, Baoji University of Arts and Sciences
Baoji, 721013, P.R. China

[b]School of Science, Xidian University, Xi'an 710071, P.R. China

[c]Nonlinear Research Institute, Baoji University of Arts and Sciences, Baoji, 721016, P.R. China

[d]Department of Physics, Northwest University, Xi'an 710069, P.R. China

(Received September 9, 2010; in final form December 20, 2010)

The crystal structure, electronic, and mechanical properties of antifluorite Be_2X (X = C, Si) are calculated using the first-principles method based on density functional theory. Our calculated lattice parameters at equilibrium volume are in good agreement with the experimental data and other theoretical calculations. In order to obtain further information, the mechanical properties including bulk modulus, shear modulus, Young's modulus, and Poisson's ratio are deduced from calculated elastic constants. Meanwhile, the sound velocity and Debye temperature are also predicted. The bonding nature in Be_2X (X = C, Si) is a complex mixture of covalent and ionic characters.

PACS: 71.15.Mb, 71.20.Nr, 78.20.Ci

1. Introduction

There has been great interest in solids formed from light elements simulated by their potential unique properties in technological and industrial applications. Some of these properties are associated with the relatively strong chemical bonding characteristic of the first row atoms, others with the frequent occurrence of large band gaps. The former leads to high melting temperature, large elastic constants, and high hardness etc. The large band gaps could lead to potential optical properties. Be_2X (X = C, Si) forms in the antifluorite structure, which is equivalent to that of the group-IV elemental semiconductor. Therefore, many properties of Be_2X are similar to those of group-IV counterparts. Moreover, for the small size of Be and C atoms, Be_2C is expected to exhibit large elastic moduli which are related to the hardness, and it has been found that Be_2C is even harder than SiC [1, 2]. Hence, it is a kind of very promising material for high pressure and temperature applications. In addition, Be_2C is highly resistant to radiation damage and may be used as a component of fission reactor fuels and as blanket materials for fusion reactors [3, 4]. Most of interest to us is that the $Be_2B_xC_{1-x}$ alloy in the antifluorite structure is predicted as possible superconductor with Be_2C as starting materials [5].

However, there are few empirical data and theoretical calculations on the physical properties of Be_2C in general, and in the mechanical, optical, and thermal properties in particular. In part, this is due to the fact that this material tends to hydrolyze to $Be(OH)_2$ and to react with O and N. Experimentally, the electron-energy-loss studies on very small samples have been performed by Disko et al. [6]. Theoretically, several calculations [7–9] have applied different density functional methods to explore the structural, electronic, and optical properties of Be_2C. These studies suggest that Be_2C is a semiconductor with large indirect gap which is leading to potential optical applications. To our knowledge, the mechanical behaviors of Be_2X (X = C, Si) compounds are least studied, and there is a lack of reports on the thermal properties about these promising materials.

In this paper, we have carried out the first-principles calculations of Be_2X (X = C, Si) at ambient conditions and higher pressure as well. Results of the electronic, mechanical, and thermal properties are systematically presented. Our calculated results for elastic constants indicate that the antifluorite Be_2X (X = C, Si) are mechanically stable. Moreover, the coexistence of ionic and covalent bonding characteristics in Be–X bond was determined using the density of state and atomic population calculations.

2. Computational methods

The density functional theory (DFT) total energy calculations were carried out using the Vienna *ab initio* simulations package (VASP). Both generalized gradient approximation (GGA) [10 11] and local density approximation (LDA) [12, 13] for the exchange correlation potential were employed. The ion–electron interaction was described using the projected-augmented wave (PAW) method. Valence states considered in this study were including Be: $2s^2$, C: $2s^22p^2$ and Si: $3s^23p^2$. The cut-off energy for the expansion of the wave function into

* corresponding author; e-mail: qunwei@xidian.edu.cn

plane wave was 520 eV in reciprocal space. The k integration over the Brillouin zone was performed up to a $14 \times 14 \times 14$ Monkhorst–Pack [14] mesh (280 points in the irreducible wedge of the Brillouin zone were used for these compounds). Total energy changes were finally reduced by less than ≈ 1 meV/f.u. The elastic constants were calculated by evaluating the stress tensor generated small strain, the criteria for convergence of optimization on atomic internal freedoms were selected as difference in total energy within 1×10^{-5} eV/atom, ionic Hellman–Feynman forces were less than 0.001 eV/Å, and the maximum strain value was 0.2%.

3. Results and discussion

3.1. Structural and electronic properties

The series of Be_2X (X = C, Si) compounds crystallize with the cubic antifluorite structure, which can be considered as zinc-blende-like lattice and belongs to space group Fm-$3m$. The cubic unit cell is composed of twelve atoms, C atoms occupy fcc sites and each C atom is surrounded by eight Be atoms at $(\pm 1/4, \pm 1/4, \pm 1/4)$ positions. This can be clearly seen from Fig. 1. The black and red sphere in Fig. 1 represents C and Be atoms, respectively. In order to calculate the equilibrium lattice constant and bulk modulus of each compound, the total energy was calculated by variation of the volumes. The calculated total energy was fitted to the third-order Birch–Murnaghan equation of state (EOS) [15]. We determined the equilibrium structure parameter a, bulk modulus B_0, and its pressure derivatives B_0'. The calculated results were listed in Table I. The previous theoretical results and available experimental data are also listed in Table I for comparison. For Be_2C, it is clear that the calculated lattice parameter a using the GGA is in excellent agreement with the experimental data, the same parameter using LDA is only 1.4% lower than that of experiment and agrees well with other theoretical results [8, 16, 17]. For Be_2Si, there is no available experimental result. However, our predicted lattice parameter a using GGA and LDA agree well with the previously reported value of Corkill and Cohen [17], calculated using the plane wave pseudopotential (PWPP) method. In addition, the bulk modulus B_0 and its pressure derivatives B_0' of Be_2C and Be_2Si within LDA are also in good agreement with other calculations. Therefore, we believe that our calculations should be reasonable and reliable.

To gain a deep insight into the electronic structure and bonding nature of the two compounds, we calculated the band structures, total and site projected density of states (DOS), and atomic populations at ambient condition, as shown in Fig. 2, Fig. 3, and Table II, respectively. In Fig. 2, it can be seen that Be_2C shows indirect semiconductor character and its fundamental band gap is about 1.25 eV, which agrees well with the results obtained by Lee et al. [8]. However, Be_2Si is said to exhibit metallic behavior in its crystalline state due to the finite density of states at the Fermi level. Clearly, there exists significant change at the Fermi energy level between two

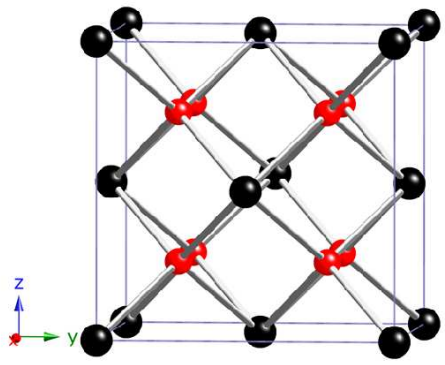

Fig. 1. The crystal structure of Be_2C, the black and red spheres represent C and Be atoms, respectively.

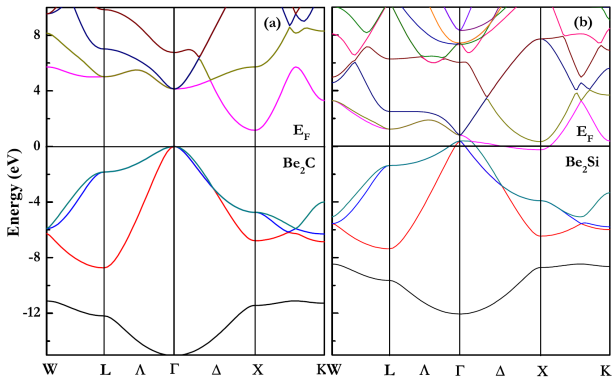

Fig. 2. The calculated band structures of the cubic (a) Be_2C and (b) Be_2Si polymorph. The position of the Fermi level is at 0 eV.

compounds, although they are in the same structure and have the similar electronic arrangement. For this discrepancy, we here provide one possible argument. The Si $3p$ orbital extends further from the nuclei than the C $2p$ orbital in Be_2C, and accordingly Si $3p$ orbital on neighboring atoms (Be) may be more overlapped than the C $2p$ orbital. This increased overlap leads to a larger inter-

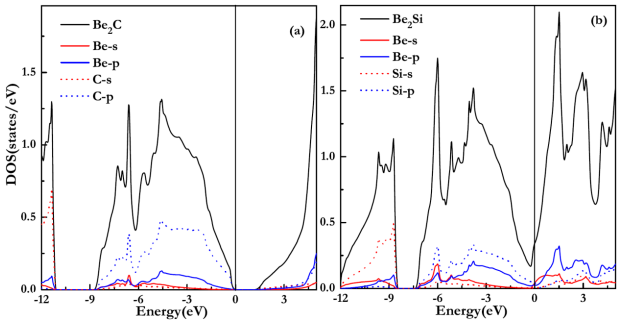

Fig. 3. The calculated total DOS and atomic projected DOS of the cubic (a) Be_2C and (b) Be_2Si polymorph. The position of the Fermi level is at 0 eV.

TABLE I

Equilibrium lattice constants a (Å), bulk modulus B_0 (GPa), and pressure derivative of bulk modulus B_0' of the Be_2C and Be_2Si.

Compounds	Method	a	B_0	B_0'
Be_2C	this work (GGA)	4.33	195.8	3.61
	this work (LDA)	4.28	213.4	3.58
	Lee et al. [8][a]	4.27	216.0	3.50
	Lee et al. [8][b]	4.29	213.0	4.18
	Laref and Laref [16][c]	4.27	217.7	3.63
	Corkill and Cohen [17][d]	4.23	216.0	
	exp. [18]	4.34		
Be_2Si	Corkill and Cohen [17][d]	5.18	103.2	
	this work (GGA)	5.28	94.5	3.64
	this work (LDA)	5.22	102.5	3.62

[a] DFT using the linear-muffin-tin-orbital (LMTO) method in the atomic sphere approximation (ASA), the exchange correlation effects are treated with LDA.

[b] The same as above, but in full potential version (FP).

[c] DFT using the full-potential linear augmented-plane wave (FPLAPW) method, the exchange correlation effects are treated with LDA.

[d] DFT using PWPP method, the exchange correlation effects are treated with LDA-CA (Ceperley and Alder) scheme.

TABLE II

Calculated atomic population of Be_2C and Be_2Si.

		s	p	d	Total	Charge [e]
Be_2C	Be (×2)	0.16	1.39	0.00	1.55	0.45
	C	1.28	3.61	0.00	4.90	−0.9
Be_2Si	Be (×2)	0.48	1.41	0.00	1.88	0.12
	Si	1.25	2.99	0.00	4.24	−0.24

action between neighbors and more bonding states are filled. Therefore, the valence bands move towards closer and even cross the Fermi level, and it can be seen distinct from Fig. 2. The calculated total and site projected DOS of Be_2X (X = C, Si) are displayed in Fig. 3, the position of the Fermi level is at 0 eV. For two compounds, the following prominent features can be seen: (i) the lower energy parts of the total DOS originate from the X s states, with minor presences of Be $2s$ states. (ii) The bonding states are mainly composed by the X $2p$ states hybridized with the Be $2s$ states near Fermi level, indicating their covalent bonding between X and Be atoms. (iii) Above the Fermi level, the principal contributions in the antibonding states come from the Be p states. In addition, we calculated the charge transfer situation between Be and X atoms by the Mulliken atomic population analysis (see Table II). The ionicity in Be–X bond is mainly featured by the charge transfer from the Be $2s$ to X p atomic orbitals in two compounds. Moreover, the number of charge transfer in Be_2C is 0.9 which is larger than that (0.24) in Be_2Si, and indicates that the Be–C bond is more ionic than the Be–Si. Therefore, the Be–X bond in two compounds displays a mixed ionic/covalent character.

3.2. Elastic and thermodynamic properties

The elastic properties express the behavior of material that undergoes stress, deforms and then recovers and returns to its original shape after stress ceases, which are usually defined by the elastic constants C_{ij}. To the best of our knowledge, almost no experimental data about the elastic properties of Be_2X are available hitherto. Thus, our results can be considered as predication for the future studies. For the present cubic Be_2X, there are three independent elastic constants, which are determined from first-principles calculations by applying a set of given homogeneous deformation with a finite value, and then calculating the resulting stress with respect to optimizing the internal atomic degree of freedom, as implemented by Milman and Warren [19]. In our calculations, we consider only small lattice distortions in order to remain within the elastic domain of the crystal. The calculated elastic constants C_{ij} are given in Table III. For a stable cubic structure, C_{ij} should satisfy the elastic stability criteria [20–22]: $C_{11}-C_{12}>0$, $C_{11}>0$, $C_{44}>0$, $C_{11}+2C_{12}>0$. Clearly, these calculated elastic constants completely satisfy the criteria, suggesting that the cubic phases Be_2C and Be_2Si are mechanically stable. For Be_2C, our calculated C_{44} value agrees very well with that obtained by Laref et al. using the FP+LAPW method. However, our calculated C_{11} and C_{12} value is larger and smaller than that obtained by the same author, respectively. Although it remains unclear for us to explain this discrepancy, we can be sure that it is not caused by the choice of the exchange-correlation potential. In fact, we have found the use of different strain in steps of 0.001 from 0.001 to 0.003 in calculations, nearly the same C_{11} and C_{12} values were obtained. We are not aware of any experimental data on the elastic constants. We hope that future experimental measurements will verify all these calculated results.

Using the calculated elastic constants C_{ij}, bulk modulus B, Young's modulus E, shear modulus G, Poisson's ratio ν, and anisotropy factor A of polycrystalline materials were determined using the Voigt–Reuss–Hill averaging scheme [23–25]. The Voigt shear modulus G_{V} and Reuss shear modulus G_{R} in the cubic system can be expressed as

$$G_{\mathrm{V}} = \frac{C_{11}-C_{12}+3C_{44}}{5}, \tag{1}$$

$$G_{\mathrm{R}} = \frac{5(C_{11}-C_{12})C_{44}}{4C_{44}+3(C_{11}-C_{12})}. \tag{2}$$

Thus, the shear modulus G is the mean value of the Voigt and Reuss moduli [25]:

$$G = \frac{G_{\mathrm{R}}+G_{\mathrm{V}}}{2}. \tag{3}$$

The bulk modulus B, Young's modulus E and Poisson's ratio ν, and anisotropic factor A can be calculated by

$$B = \frac{C_{11}+2C_{12}}{3}, \tag{4}$$

TABLE III

Elastic constants C_{ij} (GPa), bulk modulus B (GPa), shear modulus G (GPa), Young's modulus E (GPa), Poisson ratio ν, and anisotropy factor A for Be_2C and Be_2Si.

Compound	Method	C_{11}	C_{12}	C_{44}	B	G	E	ν	A
Be_2C	this work (GGA)	570.5	16.0	208.7	200.8	233.8	505.4	0.081	0.75
	this work (LDA)	602.6	22.8	221.0	216.1	246.4	535.7	0.087	0.76
	Laref and Laref [16][a]	438.3	106.4	227.2	217.1				
Be_2Si	this work (GGA)	133.0	82.5	99.0	99.3	57.6	154.8	0.26	2.1
	this work (LDA)	137.5	90.0	92.5	105.8	53.9	138.3	0.28	2.0

[a] DFT using the FPLAPW method, the exchange correlation effects are treated with LDA.

$$E = \frac{9GB}{3B+G}\,, \tag{5}$$

$$\nu = \frac{3B-2G}{2(3B+G)}\,, \tag{6}$$

$$A = \frac{2C_{44}+C_{12}}{C_{11}}\,. \tag{7}$$

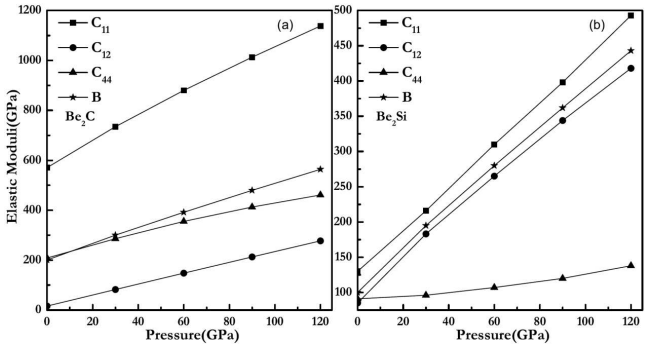

Fig. 4. The calculated pressure dependence of the elastic constants (C_{11}, C_{12}, and C_{44}) and bulk modulus B for (a) Be_2C and (b) Be_2Si.

The calculated results for these moduli, Poisson's ratio, and anisotropic factor are also listed in Table III. Let us note that we have also calculated the bulk modulus B_0 by fitting the third Murnaghan equation of states. The derived bulk modulus B is well comparable with that from the above Voigt–Reuss–Hill approximation, which again indicates that our elastic calculations are consistent and reliable. In addition, it is known that the shear modulus G of a material quantifies its resistance to the shear deformation, which is a better indicator of potential hardness for material. Remarkably, the large shear modulus of 233.8/246.4 GPa within GGA/LDA method for Be_2C, which are all larger than 197 GPa of SiC [26], indicates that Be_2C is expected to withstand shear strain to a large extent, and can be used as hard material in technological applications. For Be_2Si, the elastic constants and moduli values of which are all much smaller than those of Be_2C, may be due to its metallicity. The calculated anisotropy factor A for Be_2C and Be_2Si suggest that they are all anisotropic crystals. Additionally, the pressure dependence of the second-order elastic constants for two compounds was plotted in Fig. 4. For both Be_2C and Be_2Si, it is expected that elastic constants and bulk modulus B increase monotonically with the pressure. As far as we know, there are also no experimental or theoretical data about the pressure derivative of elastic constants for these compounds in the reported literatures. Then, our results can serve as a prediction for future investigations.

TABLE IV

The calculated longitudinal, transverse, average wave velocities (m/s), and Debye temperature (K) for cubic Be_2C and Be_2Si within GGA.

	v_t	v_l	v_m	Θ_D
Be_2C	9750	14436	10641	1677
Be_2Si	5226	9178	5808	750

In addition, the Debye temperature Θ_D was also evaluated because it is an important parameter closely related to many physical properties, such as specific, dynamic properties, and melting temperature. At low temperature, it can be calculated from the elastic constants using the average sound velocity v_m, by the following equation [27]:

$$\Theta_D = \frac{h}{k}\left[\frac{3n}{4\pi}\left(\frac{\rho N_A}{M}\right)\right]^{\frac{1}{3}} v_m\,, \tag{8}$$

where h is Planck's constant, k is Boltzmann's constant, N_A is Avogadro's number, n is the number of atoms per formula unit, M is the molecular mass per formula unit, and ρ is the density. The average sound velocity v_m is given by [28]:

$$v_m = \left[\frac{1}{3}\left(\frac{2}{v_t^3}+\frac{1}{v_l^3}\right)\right]^{-\frac{1}{3}}\,, \tag{9}$$

where v_t and v_l are the transverse and longitudinal elastic wave velocity of the polycrystalline materials and are given by Navier's equation [29],

$$v_{\mathrm{t}} = \left(\frac{G}{\rho}\right)^{\frac{1}{2}}, \tag{10}$$

$$v_{\mathrm{l}} = \left(\frac{B + \frac{4G}{3}}{\rho}\right)^{\frac{1}{2}}. \tag{11}$$

The calculated transverse and longitudinal elastic wave velocity, average sound velocity, and the Debye temperature (Θ_{D}) for two cubic compounds are given in Table IV within GGA. Our results predict that the Θ_{D} is higher for Be_2C than for Be_2Si, suggesting that Be_2C is harder than Be_2Si and supporting our expectations.

4. Conclusions

In conclusion, by performing first-principles plane--wave total energy calculations, we studied the structural, electronic, and mechanical properties of antifluorite Be_2X (X = C, Si) compounds. Our calculated equilibrium lattice constants and bulk modulus are in good agreement with available experimental data and previous theoretical results. The calculated band structures showed that Be_2C is an indirect semiconductor with a 1.25 eV band gap and Be_2Si is metal. The bonding nature of Be–X bond is a mixed ionic/covalent character, which have been fully analyzed in terms of density of states atomic population analysis. The predicted bulk modulus and shear modulus suggested that Be_2C is a hard material compared to SiC. In addition, these two compounds show different degrees of elastic anisotropy. For the first time, the Debye temperature of Be_2X (X = C, Si) was estimated to be 1677 K and 750 K at GGA level, respectively. We hope that our theoretical results could be useful for further experimental investigations.

Acknowledgments

This work was supported by Natural Science Basic Research Plan in Shaanxi Province of China (grant No. 2010JM1015), the Education Committee Natural Science Foundation of Shaanxi Province (grant No. 2010JK404), and a Baoji University of Arts and Sciences Key Research Grant (grant No. ZK0915, ZK0918).

References

[1] J.H. Coobs, W.J. Koshuba, *J. Electrochem. Soc.* **99**, 115 (1952).

[2] L.H. Rovner, G.R. Hopkins, *Nucl. Technol.* **29**, 274 (1976).

[3] E.P. Roth, *Int. J. Thermophys.* **3**, 45 (1982).

[4] H. Migge, *J. Nucl. Mater.* **103**, 687 (1981).

[5] J.E. Moussa, J. Nooffsinger, M.L. Cohen, *Phys. Rev. B* **78**, 104506 (2008).

[6] M.M. Disko, J.C.H. Spence, O.F. Sankey, D. Saldin, *Phys. Rev. B* **33**, 5642 (1986).

[7] P. Herzig, J. Redinger, *J. Chem. Phys.* **82**, 372 (1985).

[8] C.H. Lee, W.R.L. Lambrecht, B. Segll, *Phys. Rev. B* **51**, 10392 (1995).

[9] F. Kalarasse, B. Bennecer, *J. Phys. Chem. Solids* **69**, 1775 (2008).

[10] J.P. Perdew, Y. Wang, *Phys. Rev. B* **45**, 13244 (1992).

[11] J.P. Perdew, K. Burke, M. Ernzerhof, *Phys. Rev. Lett.* **77**, 3865 (1996).

[12] D.M. Ceperley, B.J. Alder, *Phys. Rev. Lett.* **45**, 566 (1980).

[13] J.P. Perdew, A. Zunger, *Phys. Rev. B* **23**, 5048 (1981).

[14] H.J. Monkhorst, J.D. Pack, *Phys. Rev. B* **13**, 5188 (1976).

[15] F. Birch, *J. Geophys. Res.* **83**, 1257 (1978).

[16] S. Laref, A. Laref, *Comput. Mater. Sci.* **44**, 664 (2008).

[17] J.L. Corkill, M.L. Cohen, *Phys. Rev. B* **48**, 17138 (1993).

[18] R.W.G. Wyckoff, *Crystal Structures*, 2nd ed., Vol. 1, Interscience, New York 1963, p. 241.

[19] V. Milman, M.C. Warren, *J. Phys., Condens. Matter* **13**, 5585 (2001).

[20] Z.J. Wu, E.J. Zhao, H.P. Xiang, X.F. Hao, X.J. Liu, J. Meng, *Phys. Rev. B* **76**, 054115 (2007).

[21] M. Born, K. Huang, *Dynamical Theory of Crystal Lattices*, Clarendon, Oxford 1956.

[22] M. Born, *Proc. Cambridge Philos. Soc.* **36**, 160 (1940).

[23] W. Voigt, *Lehrbuch der Kristallphysik*, Taubner, Leipzig 1928.

[24] A. Reuss, *Z. Angew Math. Mech.* **9**, 55 (1929).

[25] R. Hill, *Proc. Phys. Soc. London Sect. A* **65**, 350 (1952).

[26] R.D. Carnahan, *J. Am. Ceram Soc.* **51**, 223 (1968).

[27] J.R. Christman, *Fundamentals of Solid State Physics*, Wiley, New York 1988.

[28] O.L. Anderson, *J. Phys. Chem. Solids* **24**, 909 (1963).

[29] E. Screiber, O.L. Anderson, N. Soga, *Elastic Constants and Their Measurements*, McGraw-Hill, New York 1973.